



A fast on-site measure-analyze-suppress response to control vortex-induced-vibration of a long-span bridge

Lin Zhao ^{a,b,c,d}, Wei Cui ^{a,b,c,*}, Xiaomin Shen ^b, Shengyi Xu ^b, Yujun Ding ^b, Yaojun Ge ^{a,b,c}

^a State Key Lab of Disaster Reduction in Civil Engineering, Tongji University, Shanghai 200092, China

^b Department of Bridge Engineering, College of Civil Engineering, Tongji University, Shanghai 200092, China

^c Key Laboratory of Transport Industry of Bridge Wind Resistance Technologies, Tongji University, Shanghai 200092, China

^d State Key Laboratory of Mountain Bridge and Tunnel Engineering, Chongqing Jiaotong University, Chongqing 400074, China



ARTICLE INFO

Keywords:

Long-span bridge
 Vortex-induced vibration
 Field monitoring
 Vortex detection
 Spoiler

ABSTRACT

Vortex-induced vibration (VIV) occurred on Humen Bridge starting from May 5th, 2020. The direct reason was that the water-filled barriers were placed along the two edges of the bridge deck upper surface, which destroyed the streamlined aerodynamic shape configuration and, therefore, vortices were generated along the bridge section. With the help of several portable monitoring devices, wind speeds, structural motion, and airflow at the wake of the bridge section can also be recorded separately. After removing the barriers, subsequent VIV was continuing due to the decreased structural damping. The amplitude was smaller than the initial case, but still exceeded the threshold defined in Chinese bridge specification. The spoiler was proposed to be installed on the handrail to mitigate vortex and suppress VIV. The Doppler LiDAR detected that the vortex frequencies had been distorted after installing the spoiler, and bridge motion also had dramatically reduced to below the threshold when the wind climate kept as a similar condition when previous VIV happened. Therefore, the bridge administrative agency and local government decided to reopen Humen Bridge after ten days of closure.

1. Introduction

On May 5th, 2020, Humen Bridge, which crosses the Pearl River to link Guangzhou and Dongguan, occurred the large amplitude vortex-induced vibration (VIV) for the first time after 23 years of service life. Due to this emergent situation, the local government and Humen Bridge administrative office had to temporarily close the ground transportation through this bridge and the shipping channel under the bridge. Because Humen Bridge and Pearl River shipping channel are both important transportation pivots, and their closure significantly affected regional economic operation, which just started to recover slowly after the COVID-19 pandemic, and most traffic must reroute through Nansha bridge, which just opened in 2019 and now had to carry heavier traffic than designed volume.

To resolve this urgent complication, several engineering teams from various fields, including wind engineering, structural monitoring, structural design, and construction, gathered at Humen Bridge to suppress bridge excessive motion and restore the suspended traffic and navigation. After the sequential installation of aerodynamic and structural counter-VIV measures, Humen Bridge vibration amplitude reduced

from approximately 0.3 m to 0.1 m when the wind environments remain in a similar condition. Consequently, the shipping channel was reopened only two days later after bridge structural security threats were excluded, and the bridge resumed traffic only ten days when VIV was mitigated to acceptable range [1].

This study provides a detailed description of using limited available information and equipment to analyze the vibration mechanism through measurement of bridge motion, and then design and construct the necessary VIV countering measures in an efficient and timely manner. For an actual bridge located at a key point of a complex traffic network, efficient design and construction of VIV countering measures is essential and can reduce bridge closure time, financial loss, and social impact. In contrast, other traditional methods, such as wind tunnel tests and CFD simulation, would require a much longer time, which may prolong the closure of Humen Bridge. The treatment employed by Humen Bridge can be referred to as standard procedure to suppress excessive VIV of long-span bridges over the world.

* Corresponding author at: 207 Wind Engineering Building, Tongji University, 1239 Siping Road, Shanghai 200092, China.
 E-mail address: cuiwei@tongji.edu.cn (W. Cui).



Fig. 1. Geographic location of Humen Bridge.

2. Background information

2.1. Vortex induced vibration (VIV)

Vortex is periodicity generated when airflow is separated around the bluff body, then shed the wake of the body. Consequently, The fluctuating pressures around the bluff body are produced by the periodic vortex shedding, and the induced cross-wind force and torque are characterized by a dominant frequency described by the Strouhal number $St = fD/U$, where f is the dominate frequency of the vortex shedding; D is the character dimension of the bluff body; U is the mean incoming flow velocity [2].

The Strouhal number is normally determined by cross-section geometry and Reynolds number $Re = UD/\nu$, where ν is the kinematic viscosity of the airflow. For a specific bluff body, such as the deck of the long-span bridge, Re varies little in frequent natural wind $U = 0 \sim 20 \text{ m/s}$. Thus St can be approximately considered as constant, and the characteristic frequency of vortex shedding is approximately proportional to wind speed U .

When the frequency of vortex shedding is close to the fundamental frequency of flexible structures, the interaction between body and flow is both "locked-in" at a certain frequency for a small range of wind velocity, and a relatively large response occurs, such as the reported large

vibration experienced by Humen Bridge. Although normally VIV of a bridge does result in structural damages, it can disturb bridge operation and cause discomfort to vehicles' drivers and passengers [3].

Comparing with the rare on-site flutter, VIV of long-span suspension is often reported over the world, such as Deer Isle bridge in the USA [4], Great Belt Bridge in Denmark [5,6], Trans-Tokyo Bay crossing bridg in Japan [7], Xihoumen Bridge in China [8–10] and Yi Sun-sin Bridge in Korean [11]. To suppress the VIV of above bridges, various VIV-counter measures were installed on the above-mentioned bridge to suppress VIV, such as guide vanes at the bottom of the bridge deck on the Great Belt Bridge and adjustable wind barrier on Xihoumen Bridge. However, those aerodynamic measures all required detailed and long-time wind tunnel test and verification before implementation on a full-scale bridge, which is unacceptable for Humen Bridge since considerable economic loss and social impact during the bridge closure. Recently, the data-driven methods were also used to model the responses and wind loads during VIV events [12,13].

2.2. Basic information about Humen Bridge

Humen Bridge locates at the sea gate of Pearl River along the Southern coastline of China, whose coordinate is $22.791^\circ\text{N}, 113.615^\circ\text{E}$ as shown in Fig. 1. Because this region is one of the most developed metropolitan areas in China, the traffic volume was normally around 150 thousand vehicles per day in 2019, and it then has been reduced to about 90 thousand per day due to the recently opened Nansha bridge nearby.

Humen Bridge is a suspension bridge with 888 m main span, and its

Table 1
Structural dynamic characteristics of Humen Bridge after construction [14].

No.	Modal frequency (Hz)		Modal shape*	Damping ratio (%)	
	Numerical	Field test		Range	Average
1	0.0882	0.1119	SL	1.67~4.43	2.48
2	0.1117	0.1344	ASV	0.79~2.48	1.32
3	0.1715	0.1705	SV	0.56~1.37	0.88
4	0.2251	0.2325	SV	0.50~1.20	0.70
5	0.2765	0.2768	ASV	0.49~1.02	0.63
6	0.2809	0.2971	ASL	0.72~0.96	0.87
7	0.3132	0.3145	SL	0.27~0.37	0.32
8	0.3306	0.3321	ST	0.20~0.65	0.50
9	0.3682	0.3687	SV	–	–

* S: symmetric, AS: anti-symmetric, L: lateral, V: vertical, T: torsional.

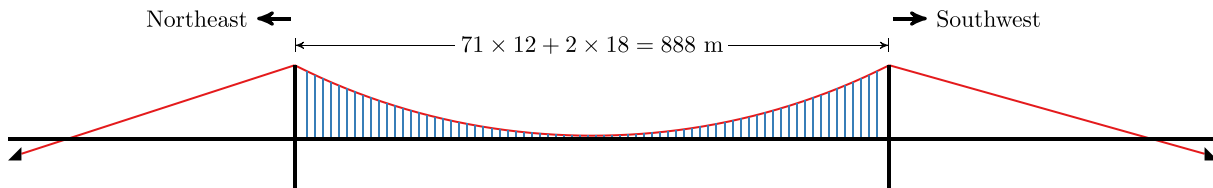


Fig. 2. Elevation view of Humen bridge geometries.

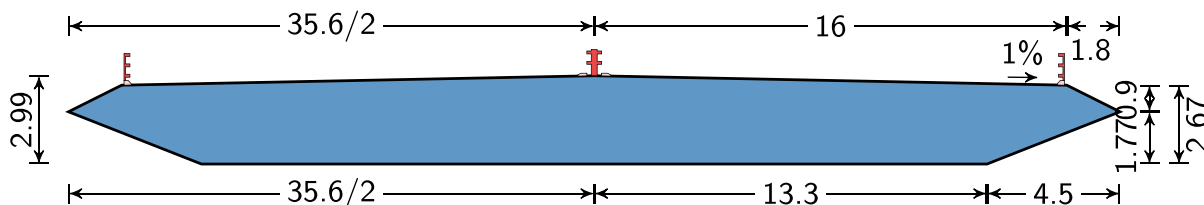


Fig. 3. Cross section of Humen Bridge deck (unit: m).

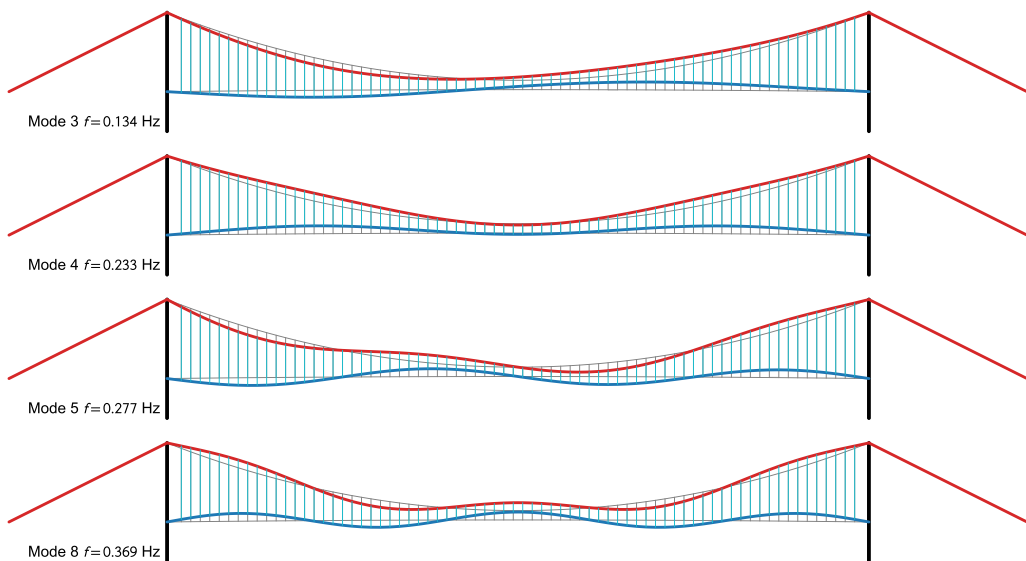


Fig. 4. Four VIV modal shapes calculated from FEM.

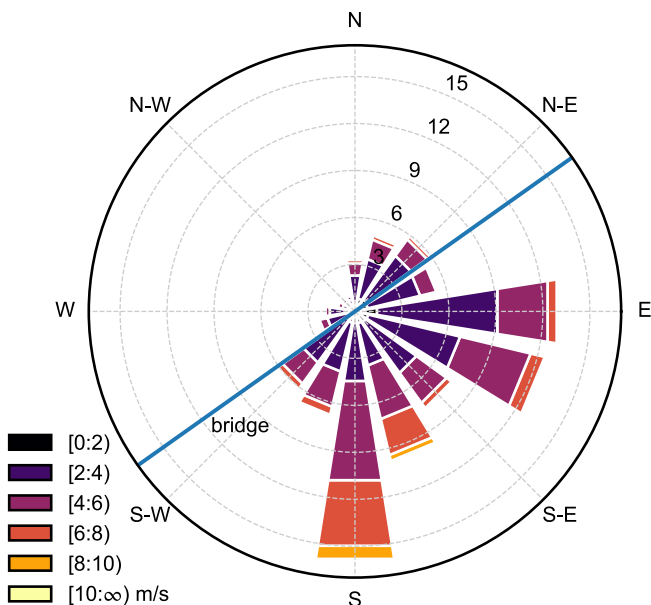


Fig. 5. Windrose at Humen Bridge site during May.

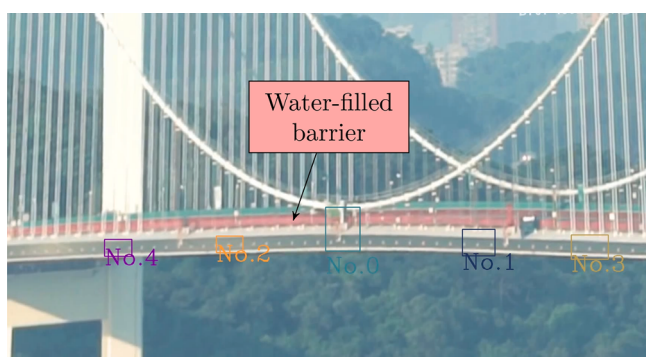


Fig. 6. Frame captured from on-line uploaded video at bilibili.com [17].

bridge towers are reinforced concrete structure. The sag to span ratio of the main cable is 1/10.5, and its two ends of the main cable are fixed by tunnel anchorages. There is a total of 72 pairs of hangers with 12 m distance. The elevation view of Humen Bridge is plotted in Fig. 2.

The streamlined closed box grid is used as the bridge deck section with 35.6 m width and 2.99 m depth, the detailed geometries of bridge cross-section is illustrated in Fig. 3.

After Humen Bridge was constructed, a field test was carried out to measure the structural dynamic characteristics [14], the structural frequency and damping were identified using half-power bandwidth method. The results are listed in Table 1.

Meanwhile, the numerical model based on finite element method was used to calculate Humen Bridge dynamic properties, and the results are also listed in Table 1 as references.

During this VIV event on Humen Bridge, there were total four modes excited by wind, and their associated modes shape are plotted in Fig. 4.

2.3. Wind climate at Humen Bridge site

Humen locates at the southern coastline of China and has a typical subtropical maritime climate, which suffers typhoon hazards during summer and strong monsoons from winter to spring. During May, the wind-rose is plotted in Fig. 5, and wind speeds and directions data are extracted from public weather data maintained by NOAA integrated surface dataset [15].

During May, most winds blow from the sector between eastern and southern. Thus there are certain winds at the speeds from 6 to 8 m/s orthogonal to the bridge span direction. This wind speed range caused the bridge VIV on May 5, 2020.

3. Causations of VIV on Humen Bridge

3.1. First observation of VIV incident

On May 5, 2020, Humen Bridge was suddenly shaking up and down violently, which was caught on camera and spread widely on social media [16]. At 15:32 local time, the bridge was shut down by traffic police for safety concerns.

In order to extract vibration mode and amplitude of Humen Bridge, the visual object tracking algorithm based on channel and spatial reliability tracking (CSRT) [18] was used. The tracking program was made based on the OpenCV framework.

The visual object tracking task is to predict the size and position of

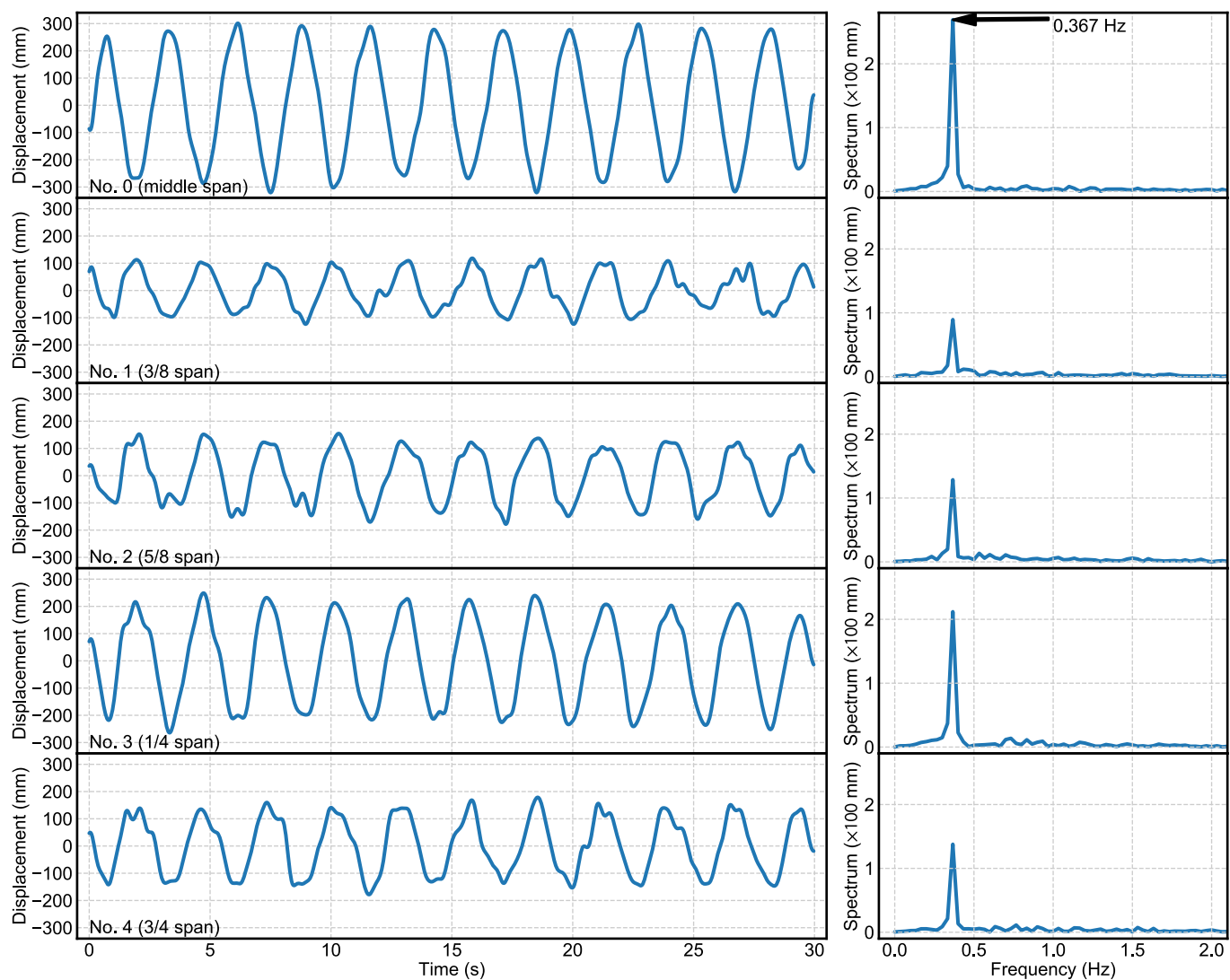


Fig. 7. Displacements at 5 locations along Humen Bridge on 2020 May 5.

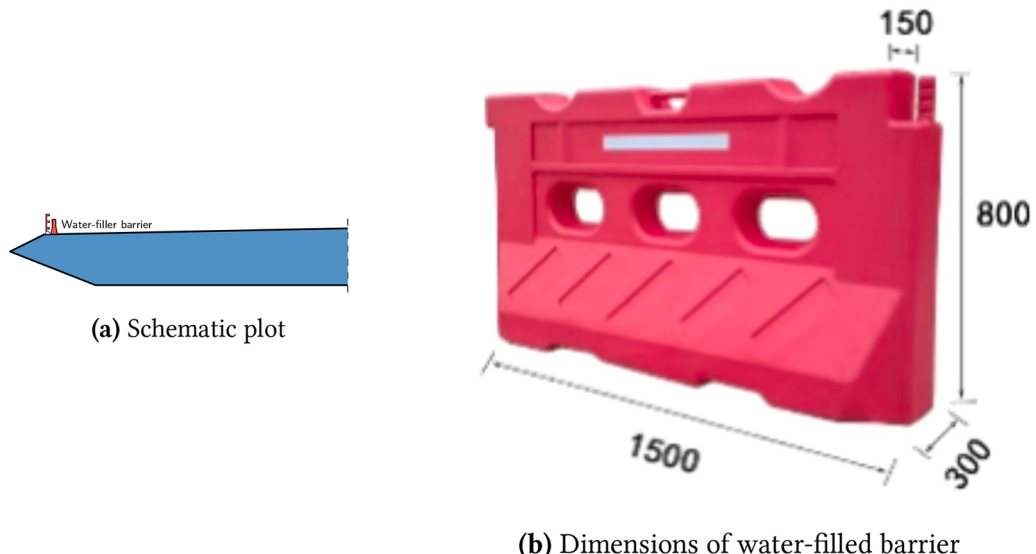


Fig. 8. water-filled barriers on Humen Bridge.

Table 2

Structural dynamic characteristics of Humen Bridge after construction.

No.	Modal frequency (Hz)		Damping ratio (%)		
	Before VIV	After VIV	Before VIV	After VIV	Reduced proportion
4	0.2325	0.230	0.70	0.26	62.9%
5	0.2768	0.276	0.63	0.28	55.5%
8	0.3687	0.367	0.50*	0.25	50.0%

* The damping value for mode 8 was missing in [14], thus the damping for mode 7 with similar frequency is used here as reference value.

the target in the subsequent frames given the size and position of the target in the initial frame of a video sequence. The algorithm logic can be described: input the initial target (Motion Model), extract the features of

these candidate frames (Feature Extractor), and then score these candidate frames (Observation Model), and finally in these ratings find the candidate box with the highest score as the prediction target (Prediction), or fuse multiple predictions (Ensemble) to get a better prediction target.

The CSRT tracking algorithm is implemented in OpenCV 4.2.0. In the first frame of the video, 5 control points were taken at the 1/4, 3/8, 1/2, 5/8, 3/4 span of Humen Bridge as the points to be tracked. Then rectangular centered on these points was drawn as the target area for algorithm tracking, which is shown in Fig. 6. The frame of 5 targets are identified frame by frame, and the pixel coordinates of the center point of those targets are extracted. Since the video comes from social media, the photographer from [17] does not provide the internal and external parameters of the camera, so it is impossible to set up the accurate

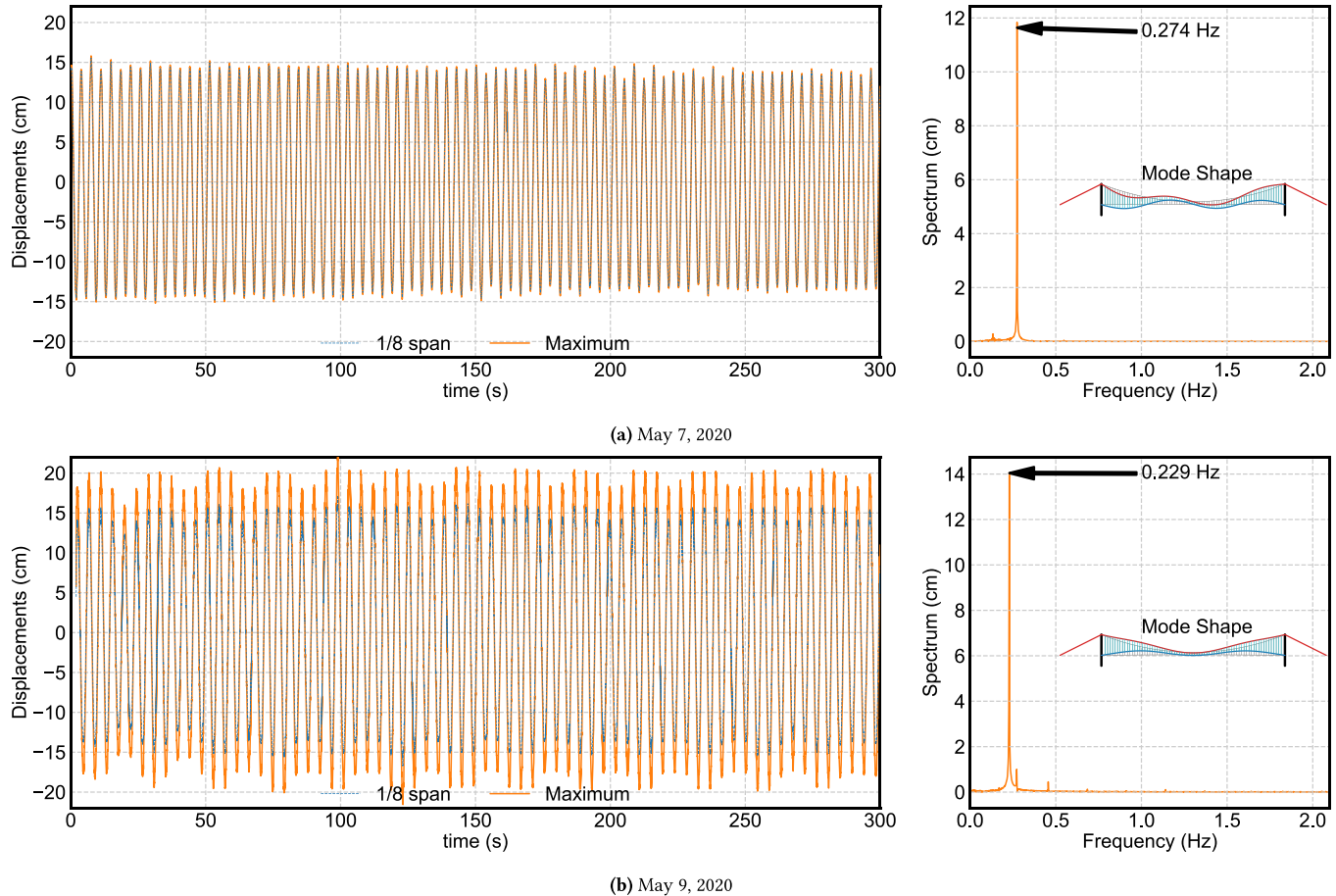


Fig. 9. VIV on Humen Bridge occurred on May 7 and May 9, 2020.

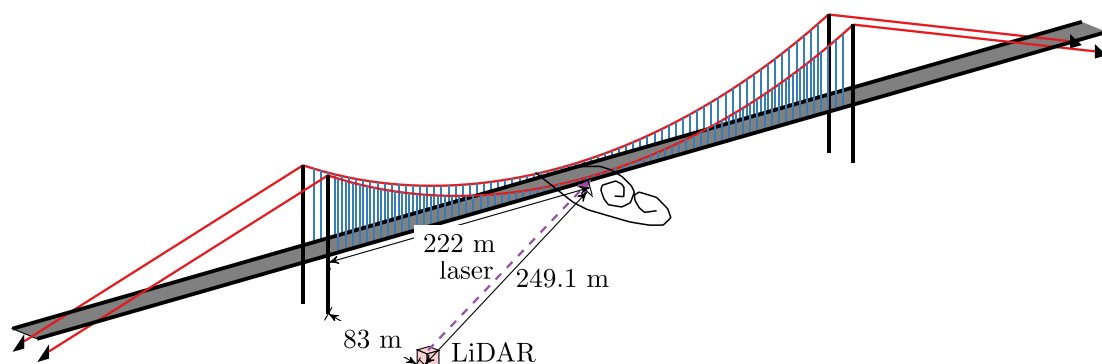


Fig. 10. Schematic plot of using LiDAR to detect vortex.



Fig. 11. Doppler LiDAR and Humen Bridge.

conversion of the pixel space to the actual scale. Therefore, the vibration time series provided in Fig. 7 only roughly converts the pixel to approximate actual length by the height of the bridge girder. The main beam of Humen Bridge is 2.99 meters high in Fig. 3, accounting for about 30 pixels in the video.

Fig. 7 shows that the vibrations at 1/4 span and 3/4 span are at the same phase, as well as the pair of 5/8 span and 3/8 span. Thus, the vibration mode is symmetric; the maximum amplitude occurred at the middle points, around 30 cm. Also, the vibration frequency matched the frequency of No. 9 mode.

Before the VIV occurred, there was an on-going hangers replacement projects and water-filled barriers with 700 mm height, shown as in Fig. 6, were placed on two sides of the bridge deck to ensure workers safety. Considering the fact that VIV has not been observed during 23 years of service time of Humen Bridge, the possible causations of this VIV incident is the alteration of the aerodynamic outline of the bridge deck due to water-filled barriers. The dimension and location of the barrier on Humen Bridge are depicted in Fig. 8. Therefore, the von Kármán type vortex was generated by those barriers and shed on the bridge deck.

3.2. Subsequent VIV incidents

After the direct reason for VIV has been identified, those water-filled barriers were removed immediately. If Humen Bridge could fully be restored to the condition before VIV on both aerodynamic and structural aspects, the VIV would decay and then disappear. However, the bridge continued to vibrate at a smaller amplitude and longer cycling-periods around 8 PM on May 5, 2020, which was also reported on several media [19]. From the direct visual observation, the amplitude has been reduced to around 20 cm, and the vibration frequency also changed to 0.27 Hz. After the removal of the water-filled barrier, the vortex frequency also changed consequently. However, it has not ever been observed that VIV occurred on Humen Bridge with the original aerodynamic shape at a similar wind condition since its construction. Thus it should be further investigated from structural dynamic aspect about the reason of this subsequent VIV phenomenon after the removal of the water-filled barrier.

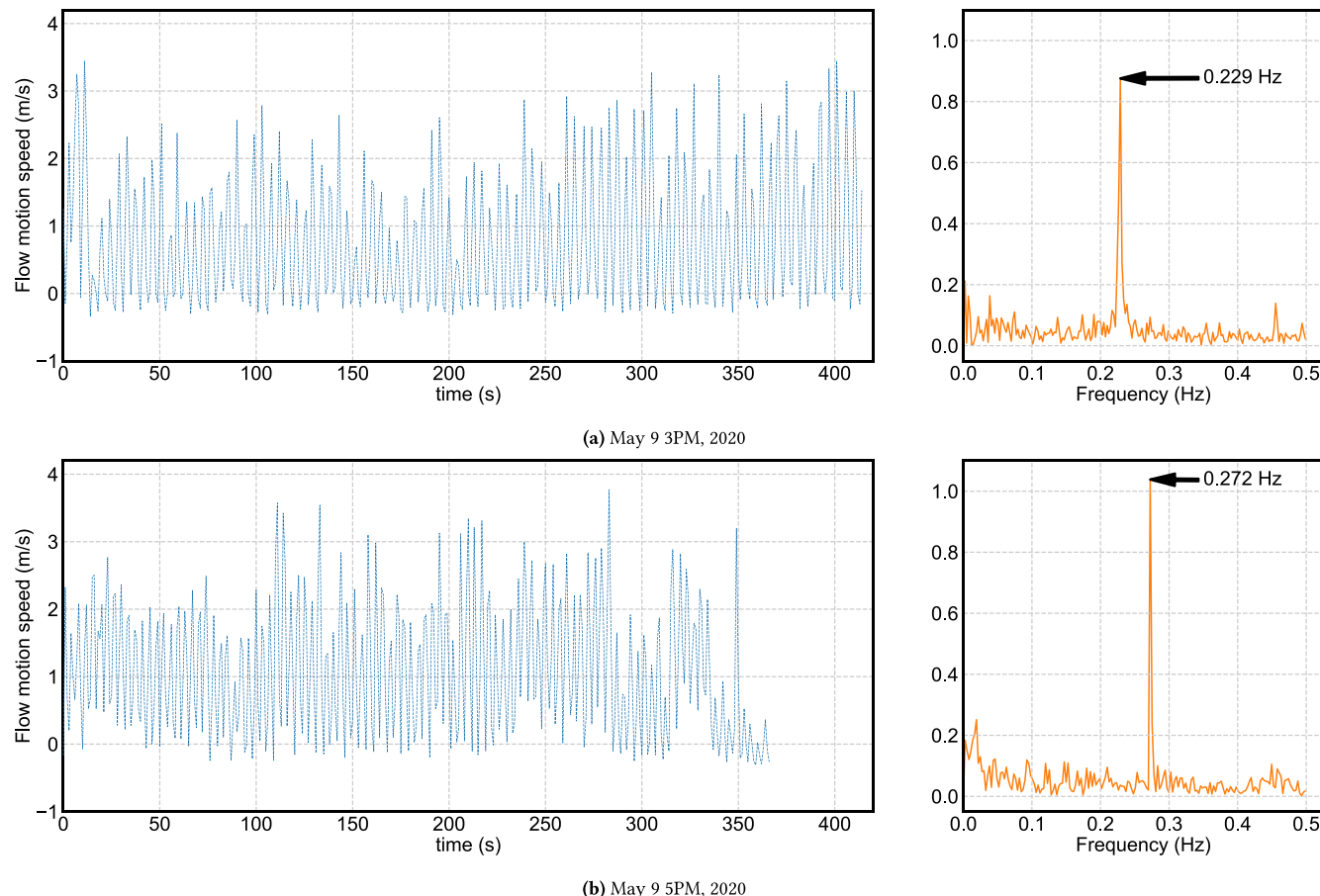
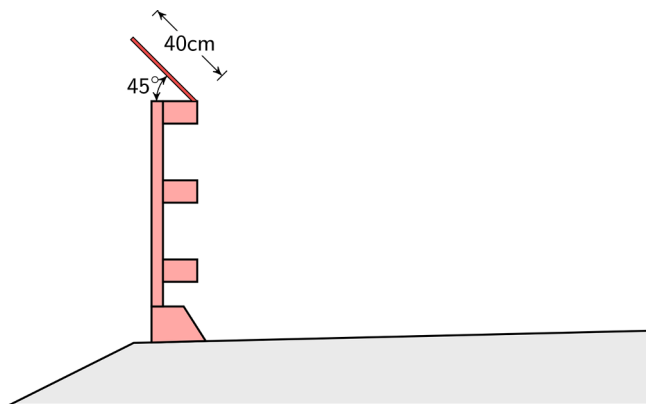
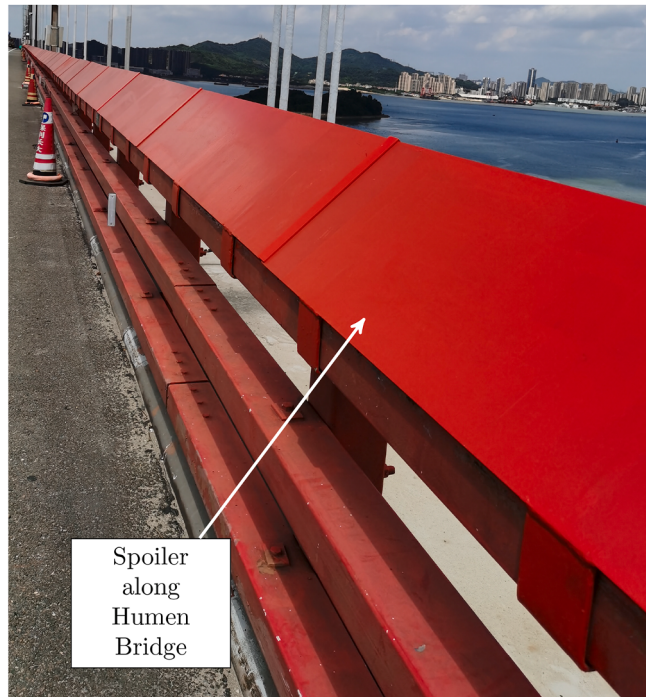


Fig. 12. Vortex frequency detected by LiDAR during VIV.



(a) Schematic plot of spoiler on the handrail



(b) Photo of spoiler on Humen Bridge

Fig. 13. Installation of spoiler on Humen Bridge.

4. Measurement of bridge motion and wake vortex

On May 7, 2020, the Tongji wind engineering team led by Prof. Yaojun Ge arrived at Humen Bridge site with several portable structural vibrations and air motion measuring devices. One day later, the structural health monitoring system started to be deployed on Humen Bridge with one 3D ultrasonic anemometer at the middle span and seven 3D accelerometers (JBA12 from Institute of Engineering Mechanics) equally spaced along the bridge. The 3D ultrasonic anemometers (YOUNG Model 81,000) produced by R. M. Young Company were employed.

4.1. Reason of subsequent VIV: structural damping plunging

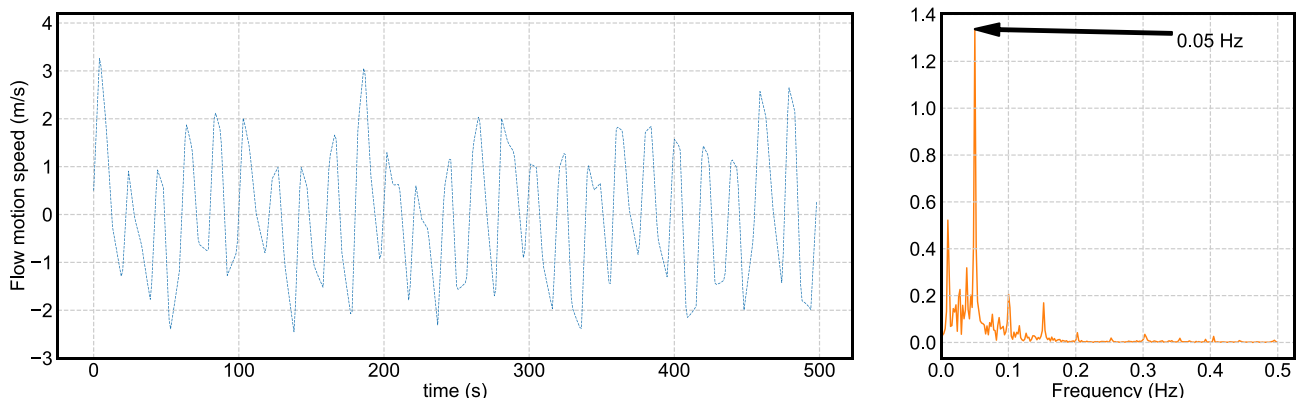
With the help of a structural acceleration monitoring system, structural dynamic modes information can be calculated when VIV was not occurring on Humen Bridge, assuming that the structure is affected by ambient environmental excitations. In this study, Bayesian FFT approach was used into identify structural frequency and damping [20]. The identified structural dynamic parameters related to VIV modes are listed in Table 2. Comparing the current status of Humen Bridge after VIV incidents with the initial status after construction, the fundamental modal frequencies keep constantly. However, the damping for each mode has been dramatically reduced to different extents. The excessive vibration due to VIV is the most likely reason for decreased damping, which was also reported in [11] about VIV occurred on Yi Sun-sin Bridge. One of the probable reasons is that frictions between the surface on structural connections were decayed due to frequent reciprocating sliding.

Therefore, although the bridge section's aerodynamic shape was restored to the original condition, Humen Bridge still continued to be vibrating due to the largely decreased damping.

Fig. 9a and b show the VIV time series and spectrum of Humen Bridge occurred on May 7 and May 9, 2020, respectively. The bridge motion was measured through a video recording device (SMTN-V multi-target tracking system produced by Beijing SITT corporation), and post-processed by sub-pixel registration algorithm [21]. The video recording camera was located exactly on the bridge deck and underneath the eastern bridge tower, and the moving targeted was chosen at 1/8 span (111 m) from the bridge tower. Because of the aerodynamic shape adjustments, the VIV frequency also changed from 0.36 Hz to 0.23 Hz or 0.27 Hz. According to the associated mode shapes in Fig. 4, the maximum amplitudes can be derived from displacements at 1/8 span.

4.2. Detecting wake vortex through air motion measurement

A Doppler LiDAR (WINDCUBE 200s produced by Leosphere) was placed below the bridge deck near the Pearl River bank to detect the air

**Fig. 14.** Vortex frequency detected by LiDAR at May 13 6PM, 2020.

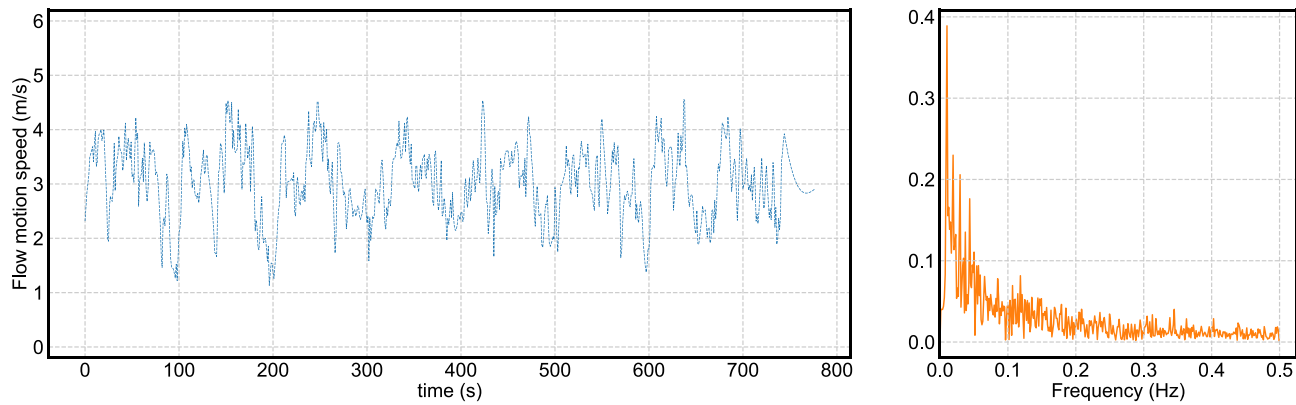


Fig. 15. Air flow spectrum detected by LiDAR at May 13 8PM, 2020.

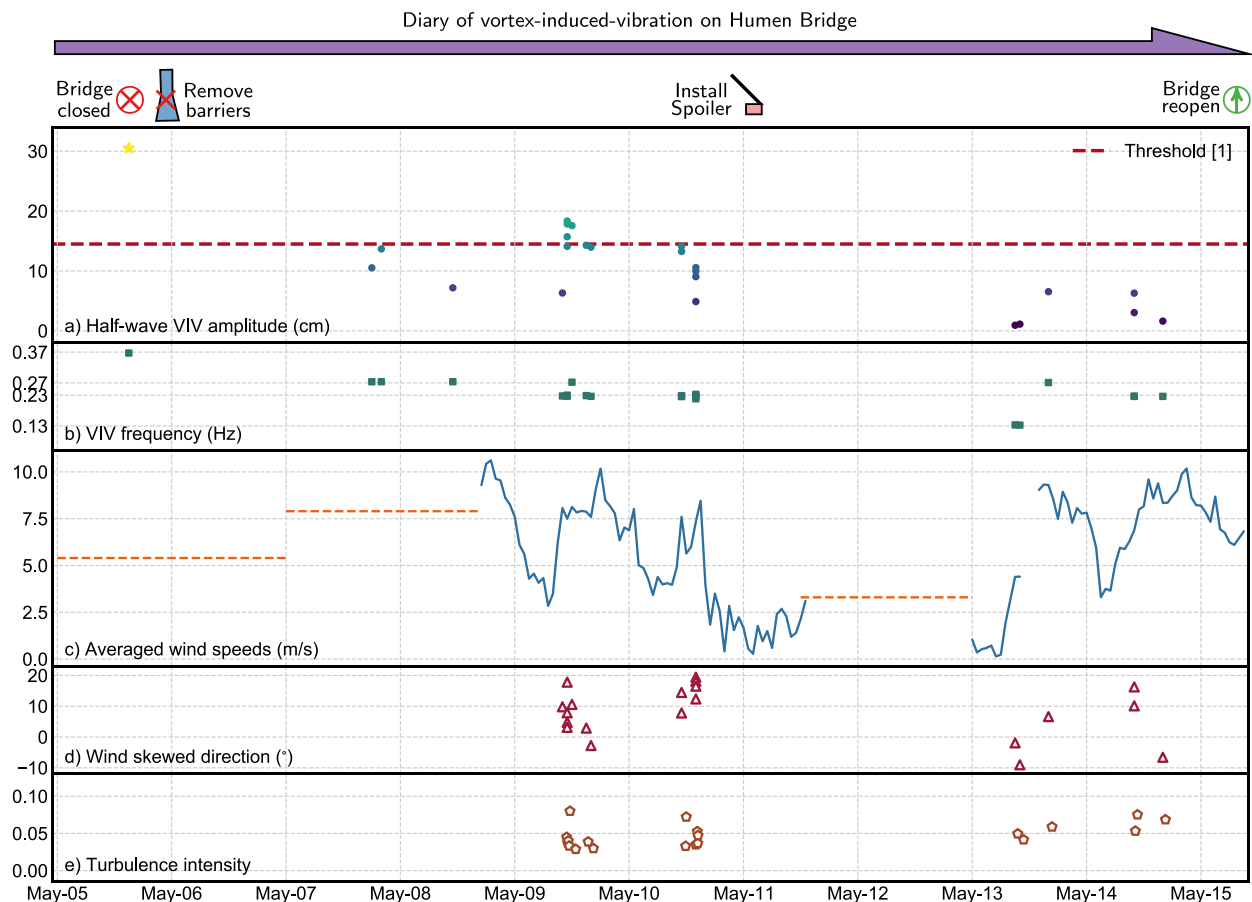


Fig. 16. Diary of emergent treatment of VIV event on Humen Bridge (a: the star indicate the initial VIV with largest amplitude on May 5, and red line is the VIV threshold defined in [1]; c: dashed line indicts that the wind speeds from anemometer were missing, thus wind speeds were estimated from public meteorological agency; d: wind skewed direction means the angle of wind direction skewed from the perpendicular line to bridge span (clockwise is positive).

motion in the wake of the bridge deck. Doppler Lidar can measure airflow speed along the laser beam based on the frequency shift due to the Doppler effect. When airflow pasted the bridge deck, the generated vortex will affect the airflow at the wake, which can be detected by Doppler LiDAR. The LiDAR was placed at 83 m away from the eastern bridge tower along the direction perpendicular to the bridge span. The laser beam was pointed at approximately the 1/8 span location. The schematic figure and photo of LiDAR are shown in Fig. 10 and Fig. 11. The two wind flow speeds samples along laser beam direction during 15 PM and 17 PM on May 9 are plotted in Fig. 12, respectively. Due to the limitation of LiDAR processing time, the sampling frequency was fixed

at 1 Hz.

Because the laser beam was not perpendicular to the bridge span direction, the wind flow cannot be directly interpreted as vortex speeds. However, its varying frequency can reflect the vortex frequency, which is also plotted in Fig. 12, and the associated frequency (0.23 Hz and 0.27 Hz) matched with the VIV frequency occurred at the same time.

5. VIV suppression through installation of spoiler on handrail

With the development of the bridge span, the bridge structure becomes more flexible. As a result, VIV is one of the major wind-induced

threats to bridge operation, driver comfortability, and structural integrity. Several aerodynamic counter-measures have been developed in recent years, such as handrail shape, air nozzle angle, wind splitter, spoiler, stabilizing plate, and guide vanes [22].

However, those counter-measures typically require the verification of the scaled bridge model in wind tunnel tests. On the real bridge, the trial-and-error procedure used in the wind tunnel cannot be implemented. Also, most methods require aerial operation outsides of paved road. Therefore, among the above mentioned regular aerodynamic counter-measures, the spoiler on the handrail is the most convenient one to be installed.

On the other hand, spoiler normally effectively reduces VIV for various bridge sections, but it is possible to increase the flutter risk during rare strong wind event [23]. Because typhoon season normally starts from July, the spoiler is an effective temporary tool to reduce VIV and even can be installed permanently if a wind tunnel test can confirm its flutter stability.

Considering the feasibility of construction materials, a 40 cm width timber plates inclined 45° outward were suggested to be installed on the surface on the handrail along two sides of Humen Bridge, but initially, only about 120 m spoiler was installed at the middle of the bridge to testify its feasibility.

The sectional view and photos of the spoiler are illustrated in Fig. 13. In the meantime, the Doppler LiDAR was also deployed to detect the vortex feature.

On May 13 6 PM, 2020, when wind speeds were around 7 m/s, and wind direction was perpendicular to the bridge span. VIV happened again but at a much smaller amplitude, and, the recorded vortex at the wake was plotted in Fig. 14. It clearly shows that the major frequency of major vortex had been transferred to 0.05 Hz, which is far away from the fundamental frequency. However, there are several small peaks at different frequencies, which indicate that VIV is still possible, but the excitation forces are at a smaller range. If the Strouhal number is assumed as a constant value, the wind speeds should reach 21 m/s to excite the bridge to vibrate at considerable amplitude, which is very rare during monsoon season. The wind flow detected by LiDAE during non-VIV events at a smaller wind speed is also plotted in Fig. 15 which shows that the spectrum peak is at a even smaller frequency, which has a different characteristic comparing with the spectrum during VIV events.

After the verification, the spoiler was extended to the full span of Humen Bridge.

After the installation of spoiler, wind became calm for two days and no VIV was observed. However, during May 13 and 14, the wind condition (wind speeds and wind directions) came back to the similar situation as May 8–May 10 when VIV occurred on Humen Bridge due to decreased damping. During this period, VIV had been detected again but with much smaller amplitude. The maximum bridge response was around 8 cm, which is below the VIV threshold given by [1]. Thus, it can be concluded that spoiler was effective to reduce VIV and Humen Bridge can be reopen to normal transporting condition.

Fig. 16 presents the dairy of emergent treatment of Humen Bridge to mitigate VIV responses. It summarizes the wind condition on Humen Bridge starting from May 9, including wind speeds, direction, and turbulence intensity. The VIV occurred during this period can roughly be divided into three groups:

1. the initial VIV occurred on May 5 with water-filled barriers (The VIV amplitude is roughly 31 cm and frequency is 0.37 Hz);
2. the VIV occurred from May 8 to May 10 when the bridge section was restored to original condition (The VIV amplitude varies from 5 cm to 19 cm with two frequencies: 0.23 and 0.27 Hz);
3. the VIV occurred from May 13 to May 14 when the spoiler has installed a handrail (The VIV amplitude varies from 1 cm to 7 cm with three frequencies: 0.13, 0.23, and 0.27 Hz).

Fig. 16 clearly states that the modifications of the aerodynamic

section shape dramatically change the VIV characteristics when the wind conditions roughly stayed the same, and the spoiler is beneficial for the VIV reduction.

6. Concluding remarks

From the VIV happening on May 5 to Humen Bridge reopen on May 15, it took ten days to analyze the causes and propose counter methods for these emergent VIV events. During this treatment, an ultrasound anemometer was used to records wind conditions. The camera recorded video was employed to display structural motion, and Doppler LiDAR was deployed to detect vortex features in the wake of the bridge section. Several important concluding remarks can be summarized:

1. the water-filled barrier is the direct causes of initial large-amplitude VIV on Humen Bridge;
2. When the bridge section was restored to original condition after removing the barrier, VIV continues at smaller amplitude due to the decreased structural damping;
3. Spoiler was effective in reducing the VIV amplitude below to threshold defined by [1] through change the vortex frequency characteristics.

Data Availability Statement

Some or all data, models, or code that support the findings of this study are available from the corresponding author upon reasonable request.

Declaration of Competing Interest

The authors declare that they have no known competing financial interests or personal relationships that could have appeared to influence the work reported in this paper.

Acknowledgments

Ph.D. Candidate Teng Ma, Department of Bridge engineering of Tongji University, was gratefully acknowledged for setting-up OpenCV framework to extract bridge motion time history from on-line video.

The authors gratefully acknowledge the support of National Natural Science Foundation of China (52008314, 51678451), Shanghai Pujiang Program (No. 19PJ1409800) and National Key research and Development Program of China (2018YFC0809604). Any opinions, findings and conclusions or recommendations are those of the authors and do not necessarily reflect the views of the above agencies.

References

- [1] Ministry of Transports of the People's Republic of China, Wind-resistant design specification for highway bridges (JTG/T 3360-01-2018), 2018.
- [2] Williamson C, Govardhan R. Vortex-induced vibrations. *Annu Rev Fluid Mech* 2004;36:413–55.
- [3] Wu T, Kareem A. An overview of vortex-induced vibration (VIV) of bridge decks. *Front Struct Civil Eng* 2012;6(4):335–47.
- [4] Kumarasena T, Scanlan R, Ehsan F. Wind-induced motions of Deer Isle bridge. *J Struct Eng* 1991;117(11):3356–74.
- [5] Larsen A, Esdahl S, Andersen JE, Vejrum T. Storebælt suspension bridge–vortex shedding excitation and mitigation by guide vanes. *J Wind Eng Ind Aerodyn* 2000; 88(2–3):283–96.
- [6] Frandsen J. Simultaneous pressures and accelerations measured full-scale on the great belt east suspension bridge. *J Wind Eng Ind Aerodyn* 2001;89(1):95–129.
- [7] Fujino Y, Yoshida Y. Wind-induced vibration and control of trans-tokyo bay crossing bridge. *J Struct Eng* 2002;128(8):1012–25.
- [8] Li H, Laima S, Ou J, Zhao X, Zhou W, Yu Y, Li N, Liu Z. Investigation of vortex-induced vibration of a suspension bridge with two separated steel box girders based on field measurements. *Eng Struct* 2011;33(6):1894–907.
- [9] Li H, Laima S, Zhang Q, Li N, Liu Z. Field monitoring and validation of vortex-induced vibrations of a long-span suspension bridge. *J Wind Eng Ind Aerodyn* 2014;124:54–67.

- [10] Ge Y, Yang Y, Cao F. VIV sectional model testing and field measurement of xihoumen suspension bridge with twin box girder. In: Proceedings of the 13th International Conference on Wind Engineering. Amsterdam, Netherlands; 2011. p. 11–5.
- [11] Hwang YC, Kim S, Kim HK. Cause investigation of high-mode vortex-induced vibration in a long-span suspension bridge. *Struct Infrastruct Eng* 2020;16(1): 84–93.
- [12] Li S, Laima S, Li H. Cluster analysis of winds and wind-induced vibrations on a long-span bridge based on long-term field monitoring data. *Eng Struct* 2017;138: 245–59.
- [13] Li S, Laima S, Li H. Data-driven modeling of vortex-induced vibration of a long-span suspension bridge using decision tree learning and support vector regression. *J Wind Eng Ind Aerodyn* 2018;172:196–211.
- [14] Zhang G, Zhu L. Test on vibration characteristics of humen bridge. *J Tongji Univ (in Chinese)*(1999);2.
- [15] Smith A, Lott N, Vose R. The integrated surface database: Recent developments and partnerships. *Bull Am Meteorol Soc* 2011;92(6):704–8.
- [16] Humen Pearl River Bridge. URL: https://en.wikipedia.org/wiki/Humen_Pearl_River_Bridge, accessed: 2020-07-02.
- [17] Video of Humen bridge vibration on 2020 May 5. URL: <https://www.bilibili.com/video/BV1Nt4y1178T/>, accessed: 2020-07-02.
- [18] Lukezic A, Vojir T, Gehovin Zajc L, Matas J, Kristan M. Discriminative correlation filter with channel and spatial reliability. In: Proceedings of the IEEE Conference on Computer Vision and Pattern Recognition); 2017. p. 6309–18.
- [19] Video of Humen bridge second vibration at nights of 2020 May 5. URL: <https://www.youtube.com/watch?v=mWRBK7O9FVs>, accessed: 2020-07-04.
- [20] Au SK. Fast bayesian ambient modal identification in the frequency domain, part i: Posterior most probable value. *Mech Syst Signal Process* 2012;26:60–75.
- [21] Tian Q, Huhns MN. Algorithms for subpixel registration. *Comput Vis Graphics Image Process* 1986;35(2):220–33.
- [22] Zhao L, Li K, Wang C, Liu G, Liu T, Song S, Ge Y. Review on passive aerodynamic countermeasures on main girders aiming at wind-induced stabilities of long-span bridges. *China J Highway Transp (in Chinese)* (2019);32(10):34–48.
- [23] Gartshore I, Khanna J, Laccinole S. The effectiveness of vortex spoilers on a circular cylinder in smooth and turbulent flow, In: Wind Engineering, Elsevier, 1980); pp. 1371–1379.